Power Control and Energetic Performances of an Induction Heating System Destined for Drying of Current Transformers

Alexandru Bitoleanu, Mihaela Popescu * and Dinu Roxan Doboşeriu
* Faculty of Electrical Engineering, University of Craiova, Craiova, Romania, alex.bitoleanu@em.ucv.ro; mpopescu@em.ucv.ro
† S.S.H. Hidroserv, Râmnicu Valcea, Romania, doboseriu_constantin@yahoo.com

Abstract - **This paper is concerned with the design of the power control system for a single-phase voltage source inverter feeding a parallel resonant induction heating load and the analyse of its energetic performances. The control of the inverter output current, meaning the active component of the current through the induction coil when the control frequency is equal or slightly exceeds the resonant frequency, is achieved by a Proportional-Integral-Derivative controller tuned in accordance with the Modulus Optimum criterion in Kessler variant. The control system response, in terms of the rms current at the inverter output when a prescribed step current is applied, shows that the dynamic and static performances are very good. In the second part, the paper presents the energetic performances of a proposed system for drying of current transformer from 110 kV Ciungetu power station. First, based on the actual technical solution and experimental recording of voltage and current, the equivalent parameters of the load circuit have been determined. In the proposed solution, the drying process is based on an induction heating system that contains a half-controlled rectifier and a voltage source inverter that operates with resonant load. The energetic performances have been determined in order to ensure zero-current switching of the inverter.**

Keywords: *Induction heating, Resonant inverters.*

I. INTRODUCTION

The voltage source inverters with resonant parallel load are used successfully in medium and high frequency induction heating systems [1]-[5]. The replacement of the current source inverters has been facilitated by both the existence on the market of the high power insulated-gate bipolar transistors (IGBTs) and the advantages of voltage source inverters [3], [5], [6]. These consist primarily in simple limiting the switching overvoltage and simplest achievement of switching at zero current. Last but not least, the use of parallel resonance allows for high load current with a small current through the inverter (only the active component). As the control system handles the operation of the induction coil in parallel with a compensation capacitor at the desired resonant frequency, the current through the induction coil is forced to be sinusoidal. In practice, the parallel resonant circuit is damped when the work piece is inserted into the induction coil by introducing additional losses into the system and increasing the current drawn from the inverter [1], [3], [5], [7].

Currently, at Hidroserv Ramnicu Valcea, the drying of the current transformers used in the high power transformer stations is carried out by a combination between the induction and conduction heating at the industrial frequency of 50 Hz.

Given the technological processes based on heating, a multifunction static system, able to provide both types of energy (DC as well as the AC) and adjust the frequency and the power level, is required, in order to obtain a high degree of flexibility [2], [3], [4]. To substantiate the feasibility of this new technical solution, the associated energetic performance assessment is needed.

For this purpose, the entire system has been modeled in Matlab/Simulink under conditions as close to reality as possible. The determination of energetic performances has been made by using parameters provided by the system design, equivalent load parameters determined based on experimental data and the controller designed in the first part of the paper.

In order to ensure zero-current switching of the inverter, the operating frequency of the square-wave inverter, which is provided by an auto-adaptive loop, is imposed to be slightly higher than the resonant frequency of the equivalent circuit consisting of induction coil-work piece in parallel with the resonant capacitor.

First, the power structure of the system and the rol of each components are presented.

The control system structure and block diagram and functions transfer are discussed in Section III. In Section IV, the control of the inverter output current is analyzed and the design of a proportional integral derivative (PID) current controller is performed based on Modulus Optimum criterion in Kessler variant. It is followed by tests on the control system performance. The energetic performances have been determined in section V and some conclusions are finally given in section VI.

II. STRUCTURE OF THE HEATING SYSTEM

The block diagram of the system for electric induction heating highlights the main components (Fig. 1).

1. Power transformer – that adapts the voltage level to the needs of the process. For the drying process, the existing transformer at Hydroserv Ciungetu will be used.

2. Half-controlled rectifier – that is part of the structure of the static voltage and frequency converter and allows the adjustment of the active power transmitted to the load.

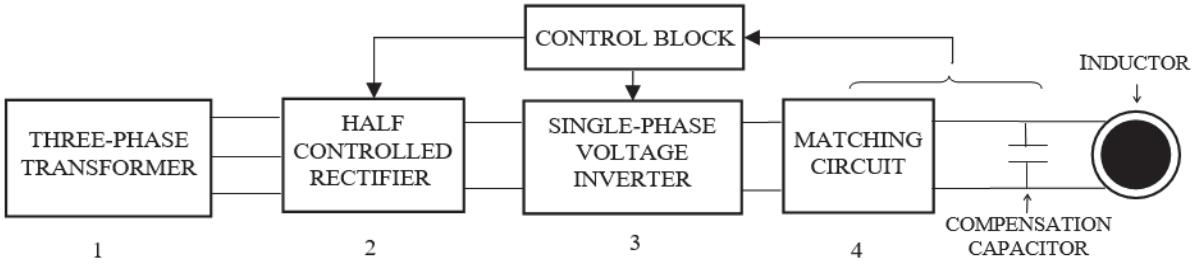

Fig. 1. Block diagram of the electric induction heating system.

3. Inverter – that converts the electrical power from DC to AC and allows the adjustment of the fundamental frequency of the load voltage, in order to obtain superior energetic performance [7] - [13].

4. Matching circuit – that is specific to the converters that supplies inductors for induction heating and aims toimprove the energetic performances. Specially, if the control frequencies are close to the resonance frequency, the matching circuit facilitates the high energetic performances [14].

The load of the heating system is the assembly consisting of inductor - heated body - compensation capacitor. It together with the matching circuit represents the load of the inverter.

In many studies of energy analysis, the components of the matching circuit, as well as the compensation capacitor, are considered ideal, lossless. Consequently, the active power at the output terminals of the inverter is equal to the active power dissipation per whole system inductor - heated piece [12], [19].

Basically, the inverter control frequency can be the resonance frequency of the equivalent circuit, the frequency that causes zero current switching, or another frequency that adjusts the power transmitted to the load.

The spectacular developing of the Isolated Gate Bipolar Transistors (IGBTs) determined the reconsideration of the voltage inverters' performances [11]-[21]. It is why, in this work, the use of IGBT-based voltage source inverter is envisaged.

III. Control System Structure And Block Diagram

The control of the current through the induction coil can be performed by controlling its active component, which means the control of the inverter output current. As regards the required value of the induction coil current, considering that the heating body is a pipe, there are two possible approaches. a) The work pipe moves through the inductor at a preset speed and the preset current depends on the required temperature gradient.

b) The maximum rated current of the voltage inverter is preset and the work pipe speed is adjusted as a function of the required temperature gradient. This is the option that allows for maximum productivity in terms of the inverter.

When the first approach is adopted, the control system requires two control loops, which are practically independent (Fig. 2).

The following blocks are highlighted in the global block diagram shown in Fig. 2: Ci – current controller; HCR – half controlled rectifier; DC – DC-link circuit; VSI – single-phase voltage source inverter; MI – matching inductor; HI – heating inductor; RC – resonant capacitor; FAB – frequency adapting block; RMS – rms value calculation; PB - protection block.

The main task of the frequency loop is to achieve the permanent and dynamic observance of the frequency, so that it is equal to or higher than the resonant frequency of the parallel circuit consisting of the equivalent inductor and the resonant capacitor, to facilitate the switching process of inverter's power semiconductors.

As the parameters of the circuit are not constant, the dynamic self adaptation of the frequency is required, by using only quantities provided by system. It results that the frequency loop cannot be controlled by external signals.

On the other hand, in order to obtain the zero-current switching of the inverter's IGBTs, the operating frequency must be slightly higher than the resonant frequency of the load circuit. Consequently, the frequency control loop must be able to achieve this second requirement too.

The block diagram in Fig. 3 illustrates the transfer functions of inverter current control loop [8].

Starting from the equivalent forward transfer function, a Proportional-Integral-Derivative (PID) controller is adopted in order to remove the dominant time constants (the constants of the DC-link circuit). The following specific constants are used: K_p, K_R and K_{Ti} – the proportional constants of the controller, rectifier and current transducer, respectively; T_i and T_d – integral and derivative controllers' time constants; T_μ - the rectifier's integral time constant which corresponds to the average dead-time associated to the firing circuit; $T_{ed} = R_d \cdot C_d$ and $T_{emd} = L_d / R_d$ - the electric and electromagnetic time constants of the DC-link circuit; $T_{ema} = L_a / R_a$ - the electromagnetic time constant of the matching inductor; $T_{eb} = R_b \cdot C$ and $T_{emb} = L_b / R_b$ - the electric and electromagnetic time constants of the parallel resonant circuit.

Note that L_b and R_b are associated to the equivalent inductance and resistance of the induction coil and heated piece and C is the capacitance of the resonant capacitor. The transducer was taken into consideration as proportional element.

In the inverter current control loop (Fig. 3), a PID controller is adopted.

Based on the Kirchhoff's laws in the Laplace domain applied to the circuit consisting in the matching induct

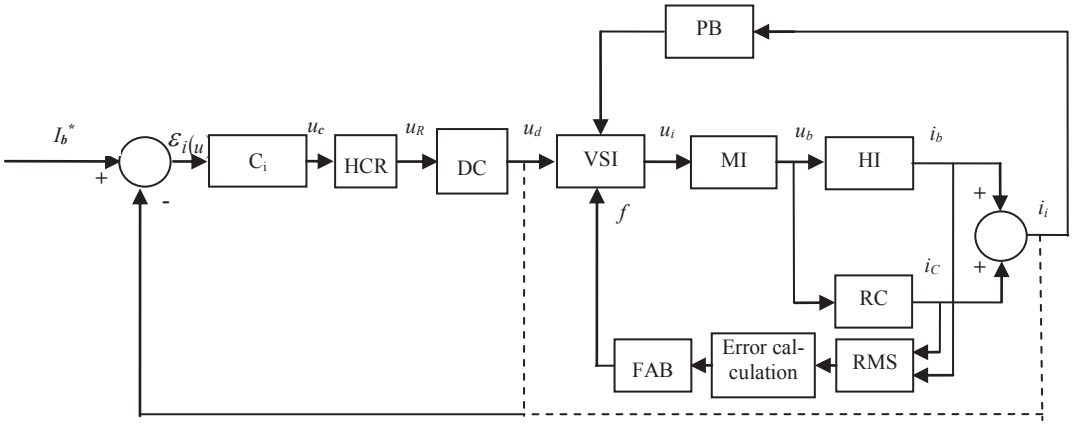

Fig. 2. Block diagram of the closed loop control system

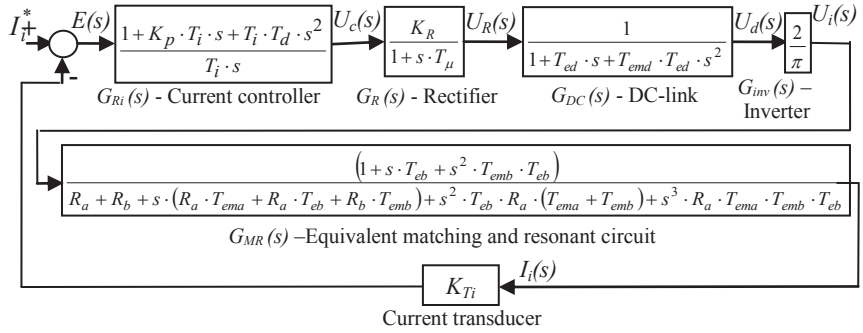

Fig. 3. Operational diagram of the inverter current control loop.

ance and the resonant capacitor in parallel with the equivalent inductor, the transfer function of the matching and resonant circuit can be expressed as follows [8]:

$$G_{MR}(s)=\frac{I_i(s)}{U_i(s)}=\frac{1}{\dfrac{R_b+sL_b}{1+sC\left(R_b+sL_b\right)}+R_a+sL_a}=$$
$$=1/R_a\cdot\left(1+T_{eb}s+T_{eb}T_{emb}s^2\right)/\left[\frac{R_b}{R_a}\cdot\left(1+T_{emb}s\right)+\right. \quad (1)$$
$$\left.+\left(1+T_{ema}s\right)\cdot\left(1+T_{eb}s+T_{eb}T_{emb}s^2\right)\right]$$

Assuming that $T_{eb}T_{emb}\ll T_{eb}$ and $R_b/R_a\ll 1$, expression (1) becomes:

$$G_{MR}(s)=\frac{1/R_a\cdot}{1+T_{ema}s} \quad (2)$$

IV. Current Controller Tuning

The current controller design is based on Modulus Optimum criterion in Kessler variant, which is dedicated to the rapid systems [8].

To reach the square modulus of the closed-loop unity feedback transfer function, the open-loop transfer function is expressed first as:

$$G_{di}(s)=G_{Ri}(s)\cdot G_R(s)\cdot G_{DC}(s)\cdot G_{inv}(s)\cdot \cdot G_{MR}(s)\cdot K_{Ti} \quad (3)$$

By using the transfer functions shown in Fig. 3 and expression (3), the following expression is obtained:

$$G_{di}(s)=\frac{1+K_pT_is+T_iT_ds^2}{sT_i}\cdot \frac{K_R\cdot(2/\pi)\cdot K_{Ti}\cdot(1/R_a)}{\left(1+sT_\mu\right)\cdot\left(1+sT_{ema}\right)\cdot\left(1+T_{ed}s+T_{emd}T_{ed}s^2\right)} \quad (4)$$

To remove the dominant time constants of the DC-link circuit, in accordance with MO criterion, two conditions are imposed in (4):

$$K_pT_i=T_{ed};\quad T_iT_d=T_{emd}T_{ed} \quad (5)$$

Thus, expression (4) becomes:

$$G_{di}(s)=\frac{K_I}{sT_i\cdot\left(1+sT_\mu\right)\cdot\left(1+sT_{ema}\right)}, \quad (6)$$

where,

$$K_I=K_R\cdot(2/\pi)\cdot K_{Ti}\cdot(1/R_a). \quad (7)$$

The integral time constant of the controller is provided by the condition of canceling the denominator term which contains a difference in the modulus square of the closed-loop unity feedback system transfer function [8]:

$$T_i=2\cdot K_I\cdot\left(T_\mu+T_{ema}\right). \quad (8)$$

When used together with (5), condition (8) gives also the expressions of the proportional and derivative constants of the PID controller:

$$K_p = T_{ed} / \left[2K_I \cdot \left(T_\mu + T_{ema}\right)\right]. \quad (9)$$

$$T_d = T_{ed} \cdot T_{emd} / \left[2K_I \cdot \left(T_\mu + T_{ema}\right)\right]. \quad (10)$$

From (8) and (10), it is found that the controller's parameters are independent of load parameters, which is an important advantage.

V. Control System Performances

To test the performances of the control system, and the energetic performances of the system, the whole induction heating system (power part and control part) has been implemented under Matlab-Simulink environment.

It includes all of the electrical components of the installation and is developed mainly with blocks from Sim Power Systems library.

To avoid using multiple Simulink models or the tandem use of the model and other MATLAB programs such as those of script type, all the needed calculation is included in the model.

Thus, after simulation, all parameters are provided (e.g. rms and average values of the quantities which are of interest, active and apparent powers, power factor, performance indicators).

The main parameters used in the Simulink model are given in Table I.

TABLE I.
The Numeric Values of the Parameters in the Simulink Model

Transformer		Rectifier		Inverter	
R_1	0.0055 Ω	Th	T62-200	IGBT	BSM200GB 120DN2
R_2	0.0055 Ω	D	1N3274	V_f	2 V
L_{s1}	52.23 µH	V_f	1.38 V	R_{on}	0.01 Ω
L_{s2}	52.23 µH	R_{on}	0.005 Ω	Fall time	10^{-7} s
M	0.1749 H	Rsnubb	500 Ω	Tail time	$2 \cdot 10^{-7}$ s
		Csnubb	0.25 µF	Rsnubb	150 Ω
				Csnubb	47 µF

It is mentioned that high accuracy results are prefigured by adopting a small simulation step in the discretized model with blocks of type switch (diodes, IGBT, etc).

The control system response, in terms of the rms current at the inverter output when a prescribed step current is applied, is shown in Fig.4 and Fig.5, in perunits.

So, the current is reported on rated value (155A) and the frequency is reported on the resonance value (2kHz). The induction coil and heated transformer parameters are R=0.122Ω and 0.946mH that have been calculated starting from experimentaly waves of voltage and current [22].

As it can be seen in Fig.4, the frequency loop searches the value that ensures zero current switching and it finds this value after 0.23 seconds. In this time, in the response of the current are identified three sequences. First, by setting the rms current of the unity value, the overshoot is of about 15% and the transient regime ends in about 0.08 seconds. Follows a second dynamic regime when the frequency closes to the zero current switching value and it finds this value. Thus, the current has an undershoot (about 20%) followed of an overshoot (about 25%).

In the Fig. 5, the conditions are:

- Initialy, the value of the equivalent inductance is increased by 25% (it means that the resonance frequency decreases about 11%) and the current is prescribed at 0.5;
- After the steady state is obtained, at t=0.4 seconds the current is prescribed at value 1;
- At t=0.5 seconds the value of the equivalent inductance becomes the rated value.

Few remarks can be drawn;

- The switching frequency has a lower steady state value; it means that the frequency loop operates properly;
- Up to t = 0.5 seconds, when equivalent inductance drops to nominal value, overtaking of current are much lower;
- After this time, the current has a big overshoot (about 65%);
- The duration of this new dynamic regime is about 0.15 seconds.

Must be underlined that the equivalent inductance value can be changed by temperature, but its change is continuously. In this conditions, the big overshoot of the current shows the sensibility of the frequency loop at changing of the inductance but cannot be really obtained.

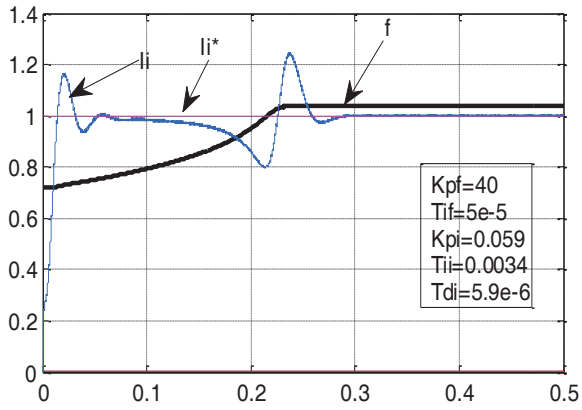

Fig. 4. Response of the inverter current and switching frequency.

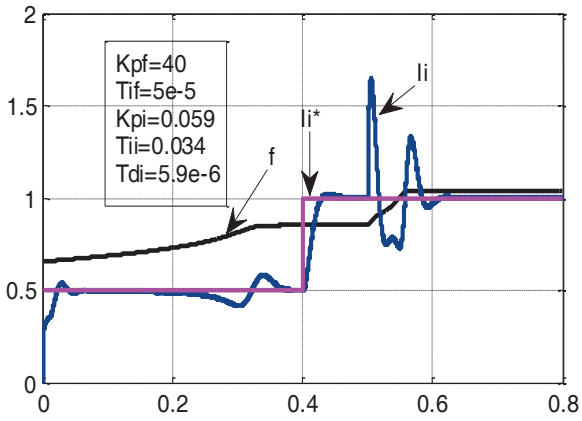

Fig. 5. Response of the inverter current and switching frequency when the prescribed current and inductance value are changed.

VI. ENERGETIC PERFORMANCES

The operation of the system in the case of prescribing the rated value of the current has been analyzed (active power of the equivalent inductor is about 15 kW). The numerical values obtained by simulation are summarized in Table II. The significance of the involved quantities is as follows:

f_{sw} - the switching frequency of the inverter;
P_s and S_s - the active and apparent powers in the transformer secondary (rectifier input);
PF_s - the power factor in the transformer secondary;
P_d - the active power at the inverter input;
η_R - the rectifier efficiency;
P_I and S_I - the active and apparent powers at the inverter output;
PF_I - the power factor at the inverter output;
η_I - the inverter efficiency;
P_{ind} - the active power across the equivalent inductor;
S_{ind} - the apparent power across the equivalent inductor;
PF_{ind} - the power factor across the equivalent inductor;
η_{ind} - the efficiency of the equivalent inductor;
η_t - the total efficiency (P_{ind}/P_s).

The analysis of the numerical results (Table II) and the waveforms in Figs. 6 shows the following:

1. The voltage in the transformer secondary is very little affected by the rectifier switches and the waveform of the current is rectangular, and its shape depends of the control angle (Fig. 6a);
2. The voltage in the DC-link circuit is practically constant and the current has pulsations (Fig. 6b);
3. The inverter output voltage is rectangular, and the current is symmetrical and nonsinusoidal (Fig. 6c);
4. The voltage across the inductor, the current through it and the current through capacitor are practically sinusoidal (rms values are equal to the fundamentals rms), (Fig. 6d);
5. The equivalent load has capacitive nature; consequently, the current flow through the compensation capacitor is higher (Fig. 6d);
6. The energetic performances are very good (the efficiencies of the rectifier, of the inverter and of the system have high values).

TABLE II.
THE ENERGY PERFORMANCES OF THE INDUCTION HEATING SYSTEM

f_{sw} [kHz]	P_s[kW]	S_s[kVA]	PFs[%]	P_d[kW]	η_R[%]	P_I[kW]	S_I[kVA]	PF_I[%]	η_I[%]	P_{ind}	S_{ind}	PF_{ind} [%]	η_{ind} [%]	η_t[%]
2.116	16.73	1087	1.54	16.51	99.4	15.45	18.16	85.1	93.42	15.02	22.58	66.53	97.21	90.26

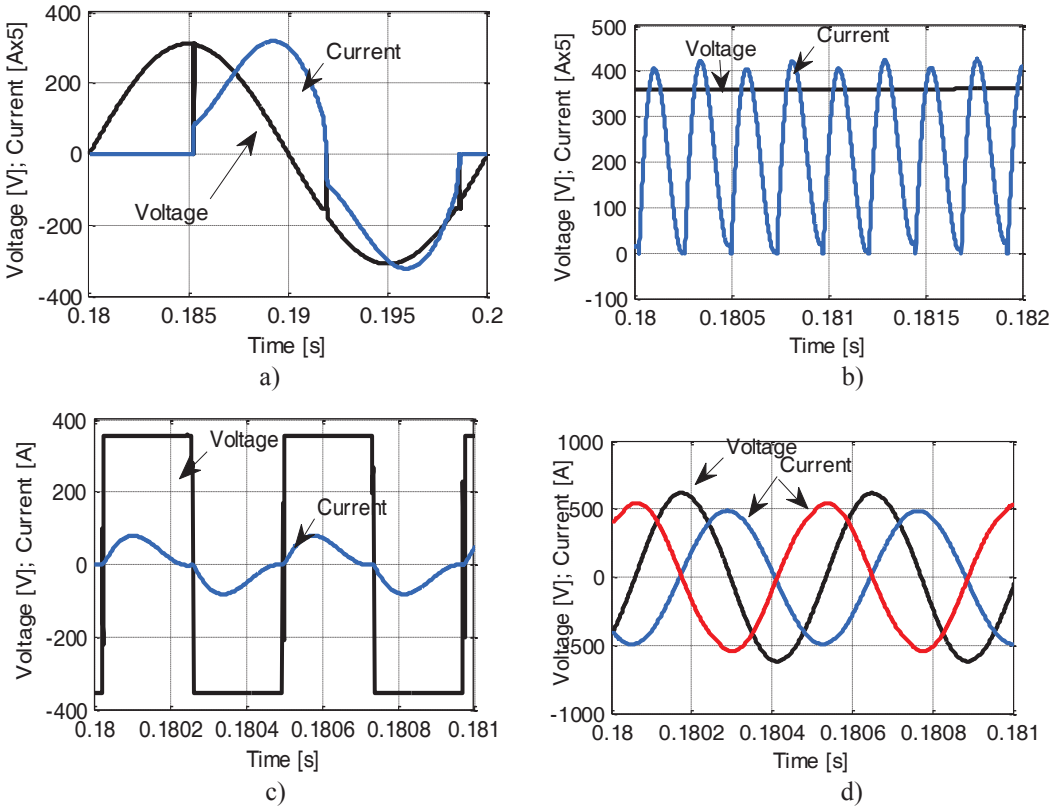

Fig. 6. Waveforms of currents and voltages when the inverter switches at zero current: voltage and current in secondary of the transformer - a); voltage and current to input of the inverter - b); voltage and current to outpu of the invertert - c); the voltage across the inductor (black), the equivalent inductor current (blue) and the current through the compensation capacitor (red) - d).

VII. CONCLUSIONS

After designing the inverter current control loop followed by the performance testing through simulation, some concluding remarks can be drawn.

1. The current controller of PID type was successfully tuned based on Modulus Optimum criterion in Kessler variant.

2. The determination of the controller's parameters is unique and leads to the elimination of inertia introduced by the DC-link circuit.

3. The tuned current controller leads to a very good performance of the current loop (the overshoot is missing or is below 25%) and the maximum duration of transient is 0.1 seconds).

4. The overshoot of the current can b e reduced if lower value of the current is prescribed (0.5 in per units) until to zero current switching frequency is stabilized.

5. The simulation results illustrate a very good behavior of the control system.

6. It has been shown that the proposed solution for drying applications in maintenance of equipment from hydroelectric plant is viable because it has very good energetic performances.

Received on July 19, 2016
Editorial Approval on November 15, 2016

REFERENCES

[1] Espi Huerta J.M.; Dede Garcia Santamaria E.J.; Garcia Gil R.; Castello Moreno J. Design of the L-LC Resonant Inverter for Induction Heating Based on Its Equivalent SRI. IEEE Trans. on Industrial Electronics[J], Vol. 54, No.6, 2007, PP:3178-3187.

[2] Espi J.M.; Dede E.J.; Navarro E.; Sanchis E.; Ferreres A. Features and design of the voltage-fed L-LC resonant inverter for induction heating. Proc. Power Electronics Specialists Conference, 1999, PP:1126 - 1131.

[3] Dieckerhoff S.; Ryan M.J.; De Doncker R.W. Design of an IGBT-based LCL-Resonant Inverter for High-Frequency Induction Heating. The 34th Industry Applications Conference, Vol. 3, Oct. 3-7, 1999, PP:2039-2045.

[4] Espi J.M.; Navarro A.E.; Maicas J.; Ejea J.; Casans S. Control circuit design of the L-LC resonant inverter for induction heating. Proc. Power Electronics Specialists Conference, 2000, PP:1430-1435.

[5] Yoo H; Shim E.; Kang J.; Choi G.; Lee C.; Bang B. 100kHz IGBT inverter use of LCL topology for high power induction heating. Proc. 8th IEEE International Conference Power Electronics and ECCE Asia, June 2011, PP:1572-1575.

[6] Salih A. IGBT for high performance induction heating applications, Proc. 38th Annual Conference on IEEE Industrial Electronics Society, Oct. 2012, PP:3274-3280.

[7] Rudnev V.; Loveless D.; Cook R.; Black M. Handbook of Induction Heating, Marcel Dekker, NY, 2003.

[8] Mihaela Popescu and A. Bitoleanu, "Power control system design in induction heating with resonant voltage inverter," in Proc. 6th International Conference on Advanced Computer Theory and Engineering, August 2013, Male.

[9] F. A. Sprânceană., D. Anghel, Metode şi procedee tehnologice. vol. II. Tehnologii Moderne, Printech, Bucuresti, 2006.

[10] M.K. Kazimierczuk, D. Czarkowski, Resonant power converters, John Wiley & Sons, 2011.

[11] A. Bitoleanu, D. Mihai, Mihaela Popescu, C. Constantinescu, convertoare statice şi structuri de conducere performante pentru acţionări electrice, Sitech, Craiova, 2000.

[12] V. Esteve, J. Pardo, J. Jordan, E. Dede, E. Sanchis-Kilders, E. Maset, "High power resonant inverter with simultaneous dual-frequency output," Power Electronics Specialists Conference, 2005, pp. 1278-1281.

[13] S. Dieckerhoff, M.J. Ruan, R.W. De Doncker, "Design of an IGBT-based LCL-resonant inverter for high-frequency induction heating," The 34th Industry Applications Conference, vol. 3, Oct. 3-7, 1999, pp. 2039 – 2045.

[14] Popescu Mihaela; Bitoleanu A.; Dobriceanu M. Analysis and Optimal Design of Matching Inductance for Induction Heating System with Voltage Inverter, The 8th International Symposium on Advanced Topics in Electrical Engineering, Bucharest, 2013, May 2013,

[15] F.P. Dawson, P. Jain, "A Comparison of Load Commutated Inverter Systems for Induction Heating and Melting Applications," IEEE Transactions on Power Electronics, vol. 6, no. 3, July 1991, pp.430-441.

[16] A. Suresh, R.S. Rama, "Parallel resonance based current source inverter for induction heating," European Journal of Scientific Research, vol. 58, no. 2, 2011, pp.148-155.

[17] Mihaela Popescu, A. Bitoleanu, E. Subţirelu, "Design and performance of the voltage control loop in induction heating systems with L-LC resonant inverters," Annals of the University of Craiova, Electrical Engineering series, No. 37, 2013, pp.39-43.

[18] S. Chudjuarjeen, A. Sangswang, C. Koompai, "An improved LLC resonant inverter for induction-heating applications with asymmetrical control," IEEE Transactions on Industrial Electronics, vol. 58, issue 7, July, 2011, pp. 2915 - 2925.

[19] P. Sreenivas, R. Vaddi, J.S. Ranganayakulu, "Full bridge resonant inverter for induction heating applications," International Journal of Engineering Research and Applications (IJERA), vol. 3, issue 1, Jan.-Feb., 2013, pp.066-073.

[20] V. Suru, Mihaela Popescu, A. Bitoleanu, "Energetic performances of induction heating systems with voltage resonant inverter," Proceedings of International Symposium on Electrical and Electronics Engineering, Galaţi, România, October 11-13, 2013.

[21] A. Bitoleanu, Mihaela Popescu, V. Suru, "Maximizing power transfer in induction heating system with voltage source inverter" The 22nd International Conference on Nonlinear Dynamics of Electronic Systems, NDES 2014, Albena, Bulgaria, June 2014.

[22] D. R. C. Doboseriu, A. Bitoleanu, M. Linca, "Energetic Performances of an Induction Heating System with Half-Controlled Rectifier Destined for Drying of Current Transformers" 2016 International Conference on Applied and Theoretical Electricity (ICATE), Craiova, Romania, 6-8 October, 2016.